Chinese Chemical Letters 34 (2023) 107780

Contents lists available at ScienceDirect

Chinese Chemical Letters

journal homepage: www.elsevier.com/locate/cclet

A novel pillar[5]arene-cucurbit[10]uril based host-guest complex: Synthesis, characterization and detection of paraquat

Yang Luo[a], Wei Zhang[a], Jie Zhao[a], Mao-Xia Yang[a], Qian Ren[a], Carl Redshaw[b], Zhu Tao[a], Xin Xiao[a,*]

[a] Key Laboratory of Macrocyclic and Supramolecular Chemistry of Guizhou Province, Institute of Applied Chemistry, Guizhou University, Guiyang 550025, China
[b] Department of Chemistry, University of Hull, Hull HU6 7RX, United Kingdom

ARTICLE INFO

Article history:
Received 26 May 2022
Revised 19 August 2022
Accepted 23 August 2022
Available online 25 August 2022

Keywords:
Pillar[*n*]arene
Cucurbit[*n*]uril
Paraquat
Supramolecular assembly
Detection

ABSTRACT

The macrocyclic family comprising pillar[*n*]arenes and cucurbit[*n*]urils have received much attention recently. However, studies on the construction of supramolecular complexes formed directly with derivatized pillar[*n*]arenes and cucurbit[*n*]urils are scant. Given the interest in such systems, herein we have synthesized a new type of naphthalene-derivatized pillar[*n*]arene NTP5 and selected Q[10] as the host molecule. The 4-[2-(1-naphthalenyl)ethenyl]pyridine of NTP5 is encapsulated by Q[10] and formed a host-guest complex in water-acetic acid (1:1) solution accompanied by enhanced fluorescence, which changed the morphology of NTP5 from a sphere to a porous form. In addition, the fluorescence of Q[10]-NTP5 can be quenched by the addition of the highly toxic pesticide paraquat (PQ), and the mechanism was shown to be the formation of a new charge transfer ternary system of Q[10]-NTP5-PQ. This work provides new ideas for the contribution of supramolecular assemblies based on derivatized pillar[*n*]arenes and their combination with cucurbit[*n*]urils and reveals their potential applications.

In recent years, pillar[*n*]arenes have received increased attention as a new type of macrocyclic molecule [1–3]. Among the numerous types of research studies conducted on pillar[*n*]arenes, the use of functionalized pillar[*n*]arenes, notably branched-chain functionalized pillar[*n*]arenes, have become particularly popular and they have been widely employed in many domains, including nanomaterials, sensing, catalysis, *etc.* [4–12]. With the development of functionalized pillar[*n*]arenes, researchers are now beginning to integrate other macrocyclic molecules, such as cucurbit[*n*]urils (Q[*n*]s) into their studies [13–18]. Stoddart and coworkers combined the advantages of cucurbit[6]uril and pillar[5]arene for the first time to construct a novel supramolecular rotaxane by making use of their rigid cavities and unique dimensions. Similarly, Huang's group has also ingeniously designed and constructed chain supramolecular polymers using pillar[6]arene and cucurbit[8]uril, where cucurbit[8]uril-enhanced π-π interactions are the main driving force. Such work demonstrates the fascination of combining two macrocyclic compounds, however surprisingly, little work has been done thus far to probe their potential applications. Moreover, most work to-date is based on the use of the same guest molecule in order to study the synergistic interaction of two macrocyclic compounds. However, in this paper, the focus of our study involves a derivatized pillar[5]arene as the guest molecule of a cucurbit[*n*]uril. The decision to employ Q[10], which has the largest cavity among Q[*n*]s found to date. As the host molecule, Q[10] is crucial because of its unique host-guest chemistry [19–24]. The huge cavity of the Q[10] can accommodate one Q[5], one calix[4]arene, two giant pyrene molecules, two tripyridine-ligated metal complexes, *etc*., and it is also very easy to bind three guest molecules to construct a unique charge transfer complex [25–30]. In addition to encapsulating large-sized molecules, Q[10]-based complexes have the unique property of enabling poorly water-soluble guest molecules to exhibit enhanced water-solubility post-assembly. This can greatly improve the performance of the assemblies as well as expanding their application prospects [31–34]. The use of Q[10] for the construction of supramolecular assemblies with functionalized pillar[5]arene will no doubt lead to unexpected effects. In addition to the construction of supramolecular assemblies based on functionalized pillar[5]arene and Q[10], some simple applications have been explored in this work.

Paraquat, also known as *N*,*N*'-dimethyl-4,4-bipyridyl dichloride (PQ), is a fast-exterminating herbicide that also can be rapidly absorbed by the green tissues of plants, causing them to die, whilst

* Corresponding author.
E-mail address: gyhxxiaoxin@163.com (X. Xiao).

https://doi.org/10.1016/j.cclet.2022.107780
1001-8417/

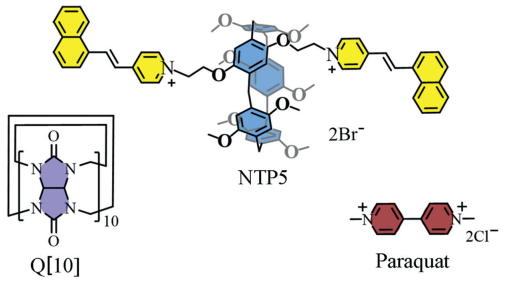

Fig. 1. The structures of NTP5, Q[10] and paraquat.

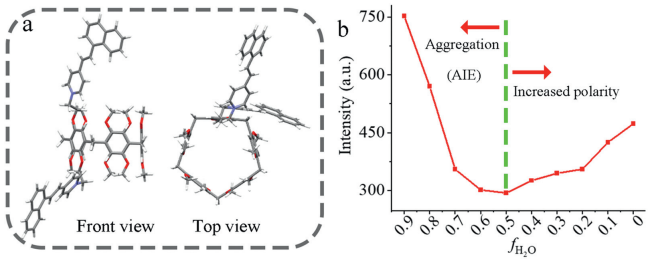

Fig. 2. The molecular modeling of NTP5 (a), gray for carbon, pale for hydrogen, blue for nitrogen and red for oxygen. The changes in fluorescent peak intensity with water fractions (b), data are extracted from Fig. S6.

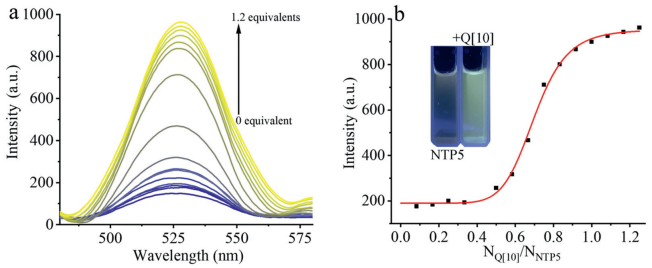

Fig. 3. (a) The fluorescence spectrum of NTP5 (20 μmol/L) in a mixed solution of water/acetic acid = 1: 1 with an increasing amount of Q[10] from 0, 0.1···1.2 equiv. at $\lambda_{ex} = 375$ nm. (b) The plot of fluorescence intensity *vs.* NQ[10]/NNTP5 at $\lambda_{em} = 527$ nm; insert: the fluorescence change observed with a 365 UV lamp.

the non-green tissues (plant roots) remain unaffected. However, this herbicide is extremely toxic to humans and has no effective antidote. Indeed, a very small dose of paraquat can reach the lethal dose for adults, and long-term skin contact with its solution can also be lethal. Paraquat is therefore banned in most parts of the world, but small amounts are still available on the market. Therefore, it is necessary to be able to detect trace amounts of paraquat [31–37].

In this work, we have designed and synthesized a novel fluorescent functionalized pillar[5]arene (NTP5, Fig. 1) using the classical fluorescent molecule 4-[2-(1-naphthalenyl)ethenyl]pyridine. Given the large size of the derivatized branched-chain of the functionalized pillar[5]arene, Q[10] (Fig. 1) was selected as the host molecule. The host-guest interaction between Q[10] with NTP5 was explored by UV–vis, fluorescence and NMR spectroscopy, and the morphology of the Q[10]-NTP5 assemblies were also characterized by means of the scanning electron microscope (SEM) and dynamic light scattering (DLS). Lastly, the Q[10]-NTP5 system was applied to the detection of paraquat and it was found that the detection level was good with a calculated detection limit of 7.06×10^{-8} mol/L. This work is more intricate than the previous Q[*n*]-based and pillar[*n*]arenes-based supramolecular polymers in terms of construction. The selection of naphthalene groups as functional groups with suitable molecular sizes not only enhances the fluorescence performance of the NTP5, but also facilitates the formation of host-guest complexes and interesting ternary supramolecular assemblies with PQ. Moreover, this work is not only limited to the construction of interesting polymers, but also involves detection studies, which will greatly promote the subsequent study of such supramolecular polymers in more depth, and provide new ideas for building supramolecular complexes based on cucurbit[*n*]urils and functionalized pillar[*n*]arenes for future applications.

NTP5 was synthesized by refluxing bromine-substituted copillar[5]arenes (DBP5) and 4-[2-(1-naphthalenyl)ethenyl]pyridine in DMF for 2 days (Scheme S1 in Supporting information). Due to the large modified groups of NTP5, it no longer has a high degree of symmetry, which makes crystal preparation difficult. However, with the help of computational chemistry, the simulated structure of NPT5 was obtained *via* the semi-empirical method GFN2-xTB. As shown in Fig. 2a, NTP5 retains the characteristic columnar cavity of the pillar[*n*]arenes, but the modified 4-[2-(1-naphthalenyl)ethenyl]pyridine group flips due to a large steric effect. In terms of solubility, although NTP5 is modified by two quaternary ammonium groups, its water solubility is still poor, but it has good solubility in polar solvents such as acetic acid. In addition, NTP5 also retains the unique aggregation-induced emission (AIE) effect of a pillar[*n*]arene in macrocyclic molecules (Fig. S6 in Supporting information) [38]. NTP5 displays a weak yellow fluorescence at 350 nm excitation in 50% water (water:acetic acid = 1:1), while in 90% water, NTP5 exhibits strong fluorescence properties due to its aggregation in insoluble solvents, resulting in the well-known restricted intramolecular rotation (RIR). Meanwhile, the fluorescence intensity decreases with increasing water content from 0 to 50% (Fig. 2b), which is due to the change in solution polarity (Figs. S7 and S8 in Supporting information) [39–41]. The interesting AIE effect of NTP5 enables NTP5 to exhibit good fluorescence properties in the aggregated state, which means that fluorescent materials, fluorescent sensors, *etc.*, with more application potential can be prepared *via* the self-assembly of NTP5.

The interaction between NTP5 and Q[10] in a mixture of acetic acid and water solvents (v/v = 1:1) was first studied by fluorescence titration, because the fluorescence of NTP5 was very weak under these conditions and the fluorescence changes were more easily observed. As seen in Fig. 3, the fluorescence change of NTP5 after the addition of Q[10] can be divided into three stages, *i.e.*, flat, rising, and flat. When the molar ratio of Q[10]:NTP5 was below 1:2, the fluorescence intensity of NTP5 grew very slowly. When the ratio exceeded 1:2, the fluorescence intensity of NTP5 started to increase sharply from 148 a.u. to 965 a.u. ($\Delta I = 817$ a.u.), indicating that NTP5 starts to aggregate at this point ($N_{Q[10]}$:$N_{NTP5} = 1:2$). When the molar ratio continued to rise to 1:1 (Q[10]:NTP5), the rising trend of the fluorescence intensity of NTP5 started to level off, indicating that the aggregation of NTP5 had reached saturation. The above fluorescence experiments showed that the interaction ratio of Q[10] and NTP5 is 1:1.

To better understand the interaction between Q[10] and NTP5, NMR spectroscopic titrations were carried out. Considering the solubility of Q[10] and NTP5, we carried out ^{1}H NMR spectroscopic experiments in a mixture of D_2O and DMSO–d_6. Due to their poor solubility in the mixed solutions, the proton signal peaks of NTP5 and Q[10] are very weak and difficult to distinguish. Nevertheless, NMR spectroscopy still provides a generalized interpretation of the host-guest interactions (Fig. S9 in Supporting information). With increasing Q[10], it can be seen that the proton signals of the 4-(1-naphthylenevinyl)pyridine of NTP5 (δ 6.95–8.62) as a whole shift considerably upfield (δ 6.37–6.88), while that of the benzene ring of NTP5 shifts downfield from 6.56 ppm to 6.72 ppm. At the same time, the proton signals of the Q[10] split significantly, with the

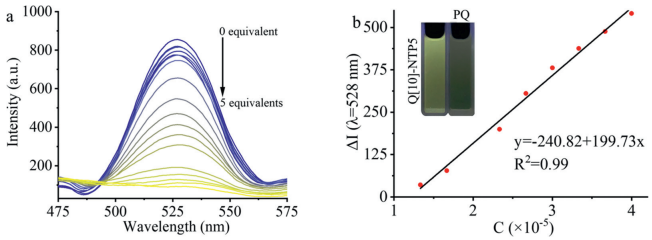

Fig. 4. (a) The fluorescence spectrum of Q[10]-NTP5 in a mixed solution of water/acetic acid = 1:1 with an increasing amount of PQ from 0, 0.2⋯ 5 equiv. at λ_{ex}= 375 nm; (b) The plot of ΔI *vs.* C_{PQ}, inserting the fluorescence change observed with 365 UV lamp.

peak at δ 5.67 changing from a doublet into a triplet peak and the peak at δ 5.25 splitting into multiple peaks. The above changes in chemical shifts and the splitting of the proton peak suggest that the Q[10] interacts with NTP5 through host-guest interactions and that the large cavity of the Q[10] tightly binds with the 4-[2-(1-naphthalenyl)ethenyl]pyridine group of NTP5. Subsequently, UV–vis spectroscopy was further applied to study the electronic transition of NTP5 (Fig. S10 in Supporting information). NTP5 has a strong absorption peak at 288 nm caused by the π-π^* transition and a weak absorption peak at 395 nm caused by the n-π^* transition. As the amount of Q[10] increased, the absorption peak of NTP5 at λ = 288 and λ = 395 nm decreased and then increased with an inflection point of 1:1, which is mainly due to the π-π^* and n-π^* transition caused by the hydrophobic effect of the Q[10] cavity. The above series of electron transfer changes are caused by the host-guest interactions between Q[10] and NTP5, consistent with the previous observations.

Q[10] form π-π^* and n-π^* electron-transition supramolecular complexes with NTP5, which makes the Q[10]-NTP5 complexes possess good fluorescence properties and can be applied to the detection of small organic compounds. Paraquat, as a classical guest molecule of both cucurbit[n]uril and pillar[5]arene is also a very harmful pesticide to humans, hence it is very important that it can be detected. The Q[10]-NTP5 complex proved to exhibit a good detection performance for paraquat. As shown in Fig. 4, it was found that the dropwise addition of a paraquat solution to the Q[10]-

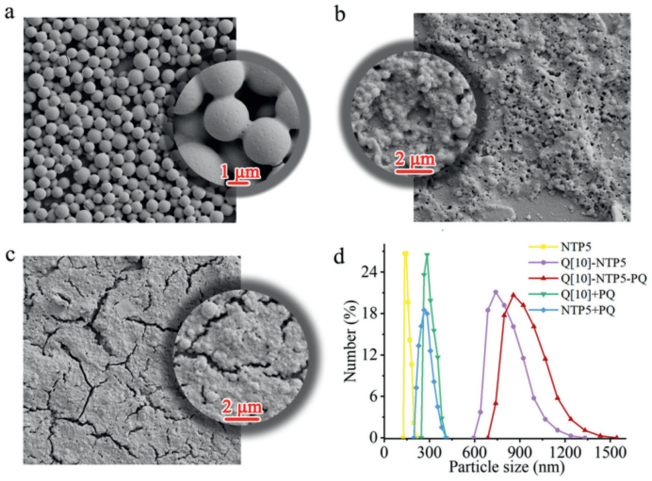

Fig. 6. The SEM of (a) NTP5; (b) Q[10]-NTP5; (c) Q[10]-NTP5-PQ, insert for the morphological details and the red line is the corresponding ruler. (d) The DLS of NTP5 (yellow), Q[10]-NTP5 (purple), Q[10]-NTP5-PQ (dark red), Q[10]-PQ (green), NTP5-PQ (blue), and the detailed DLS data are also presented in Table S1 (Supporting information).

NTP5 complex rapidly and sharply quenched the fluorescence of the Q[10]-NTP5 complex, and the fluorescence intensity dropped directly from 800 a.u. to 100 a.u. Meanwhile, the change in fluorescence from yellow to colorless can also be observed in the cuvette, which indicates that the test can be observed by the naked eye. The detection limit was calculated to be 7.06×10^{-8} mol/L using the formula $y = -240.82 + 199.73x$ to fit a good straight line.

^{1}H NMR spectroscopic titrations were then used to investigate the detection mechanism. Normally, paraquat can enter the cavity of a conventional pillar[5]arene. However, in this case, the portals of NTP5 have been modified with the large derivative branched chains of (4-[2-(1-naphthalenyl)ethenyl]pyridine), which may prevent the paraquat from entering the cavity (Fig. S13 in Supporting information). After adding paraquat, the proton signals of paraquat shifted to low fields, suggesting that the derivatized branched chains (4-[2-(1-naphthalenyl)ethenyl]pyridine) in-

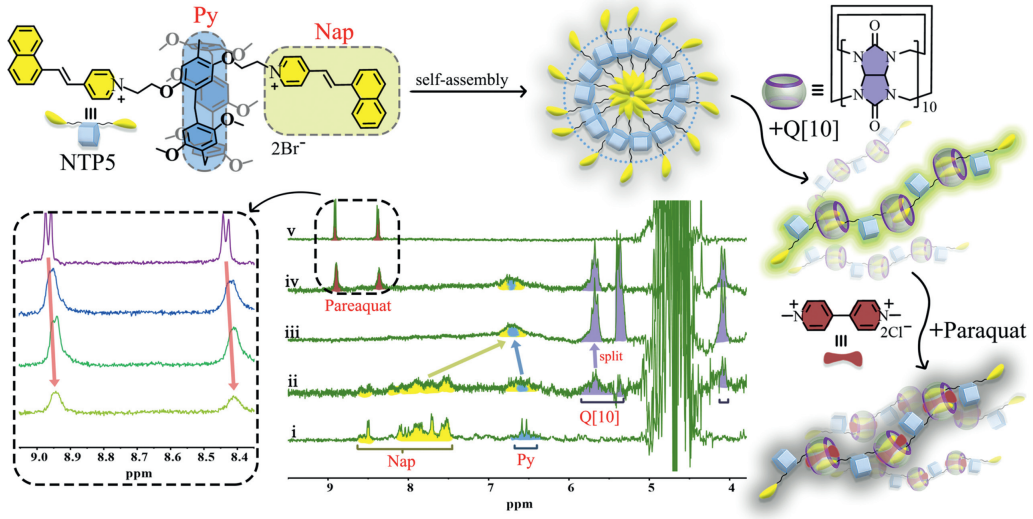

Fig. 5. Illustration (top) of the interaction of NTP5, Q[10]-NTP5, Q[10]-NTP5-PQ and the ^{1}H NMR spectrum (bottom) of (i) 0.5 mmol/L NTP5, (ii) Q[10]-NTP5 (1:2, C_{NTP5} = 0.5 mmol/L), (iii) Q[10]-NTP5 (1:1, C_{NTP5} = 0.5 mmol/L), (iv) Q[10]-NTP5-PQ (1:1:2, C_{NTP5} = 0.5 mmol/L), (v) 1 mmol/L PQ in 90% D_2O of DMSO–d_6, insert is Q[10]-NTP5 at different concentrations of PQ (Fig. S12 for full spectrum). Color marking of proton signal peaks: yellow for the 4-[2-(1-naphthalenyl)ethenyl] pyridine group of NTP5, blue for the benzene rings of NTP5, purple for Q[10], and dark red for paraquat.

deed prevented the paraquat from entering the cavity. Therefore, the use of ^{1}H NMR spectroscopic titration experiments on the Q[10]-NTP5 complex and paraquat is crucial for elucidating its mechanism. As shown in Fig. 5, on the addition of paraquat, the proton signal of paraquat is slightly displaced to high fields, and the proton signals of the Q[10]-NTP5 assembly were not significantly affected, which means that paraquat enters the huge cavity of Q[10] rather than that of NTP5. Therefore, it can be inferred that the decline of fluorescence caused by the addition of paraquat is due to the construction of the classic charge transfer complex of Q[10]-NTP5-PQ [26,27,42-44]. In addition to NMR spectroscopy, we also employed DLS and SEM to corroborate the finding of the charge transfer complex (Fig. 6). The results of DLS indicate that both Q[10]-NTP5 (740 nm) and Q[10]-NTP5-PQ (857 nm) have larger particle sizes than NTP5 (137 nm) and NTP5-PQ (265 nm), indicating that paraquat not only did not dissociate the Q[10]-NTP5 assembly into monomers but that it also further contributed to the formation of the charge-transfer complex. The structure of Q[10]-NTP5-PQ has also been subjected to quantitative calculations to confirm its credibility. SEM and TEM (Fig. S14 in Supporting information) were able to confirm the formation of ternary complexes and visualize the above-mentioned complexes. NTP5 in the solid-state is a more homogeneous sphere (Fig. 6a), while the addition of Q[10] makes the spheres sparse without obvious contours and somewhat porous in structure (Fig. 6b). After the addition of paraquat, the whole shape becomes very compact and uneven spherical particles can be observed at the outer surface of these compact structures (Fig. 6c).

4-[2-(1-Naphthalenyl)ethenyl]pyridine was used to design and synthesize a new type of pillar[*n*]arene, namely NTP5. Due to its larger size, Q[10] was selected as the host molecule, and their host-guest interaction was investigated. It was found that Q[10] greatly improved the fluorescence performance of NTP5 by restricting its intramolecular rotation. Subsequently, Q[10]-NTP5 was used to detect highly toxic paraquat and good results were achieved, with the addition of paraquat promoting the formation of the charge-transfer complex. The work in this paper provides new insights into the derivatization of pillar[*n*]arenes and their combination with cucurbit[*n*]urils and reveals that such systems have potentially useful applications, such as the construction of novel supramolecular polymers *via* two macrocyclic host molecules, as well as utilizing these polymers for specific molecular recognition, bioimaging.

Declaration of competing interest

There are no conflicts of interest.

Acknowledgments

This work was supported by the National Natural Science Foundation of China (No. 21861011), the Innovation Program for High-level Talents of Guizhou Province (No. 2016-5657), and the Science and Technology Fund of Guizhou Province (No. [2020]-1Y046). Carl Redshaw thanks the University of Hull for support.

Supplementary materials

Supplementary material associated with this article can be found, in the online version, at doi:10.1016/j.cclet.2022.107780.

References

[1] T. Ogoshi, S. Kanai, S. Fujinami, T. Yamagishi, Y. Nakamoto, J. Am. Chem. Soc. 130 (2008) 5022–5023.
[2] M. Xue, Y. Yang, X. Chi, Z. Zhang, F. Huang, Acc. Chem. Res. 45 (2012) 1294–1308.
[3] P.J. Cragg, K. Sharma, Chem. Soc. Rev. 41 (2012) 597–607.
[4] E. Lee, H. Ju, I.H. Park, et al., J. Am. Chem. Soc. 140 (2018) 9669–9677.
[5] J.F. Chen, X. Yin, B. Wang, et al., Angew. Chem. Int. Ed. 59 (2020) 11267–11272.
[6] A.J. Savyasachi, O. Kotova, S. Shanmugaraju, et al., Chem 3 (2017) 764–811.
[7] J.R. Wu, Y.W. Yang, Angew. Chem. Int. Ed. 60 (2021) 1690–1701.
[8] Y. Cao, Y. Chen, Z. Zhang, et al., Chin. Chem. Lett. 32 (2021) 349–352.
[9] J. Wang, M. Cen, J. Wang, et al., Chin. Chem. Lett. 33 (2022) 1475–1478.
[10] B. Lu, Z. Zhang, Y. Ji, et al., Sci. China Chem. 65 (2022) 1134–1141.
[11] L. Xia, J. Wu, B. Huang, et al., Chem. Commun. 56 (2020) 11134–11137.
[12] L. Xia, J. Tian, T. Yue, et al., Adv. Healthcare Mater. 11 (2022) 2102015.
[13] J. Yang, L. Shao, J. Yuan, F. Huang, Chem. Commun. 52 (2016) 12510–12512.
[14] C. Ke, N.L. Strutt, H. Li, et al., J. Am. Chem. Soc. 135 (2013) 17019–17030.
[15] T. Ogoshi, R. Shiga, T. Yamagishi, J. Am. Chem. Soc. 134 (2012) 4577–4580.
[16] D. Zhang, H. Tang, G. Zhang, L. Wang, D. Cao, Chem. Commun. 57 (2021) 6562–6565.
[17] T. Zhang, Y. Liu, B. Hu, et al., Chin. Chem. Lett. 30 (2019) 949–952.
[18] Y. Yang, X.L. Ni, J.F. Xu, X. Zhang, Chem. Commun. 55 (2019) 13836–13839.
[19] M. Cao, F. Hu, X. Han, et al., Chin. J. Chem. 33 (2015) 351–355.
[20] Y. Luo, S. Gan, W. Zhang, et al., Mater. Chem. Front. 6 (2022) 1021–1025.
[21] W.T. Xu, Y. Luo, W.W. Zhao, et al., J. Agric. Food Chem. 69 (2021) 584–591.
[22] F. Liu, S. Chowdhury, R. Rosas, et al., Org. Lett. 23 (2021) 5283–5287.
[23] G. Fan, X. Yu, X. Han, Z. Zhao, S. Liu, Org. Lett. 23 (2021) 6633–6637.
[24] H. Wang, Y. Yang, B. Yuan, et al., ACS Appl. Mater. Interfaces 13 (2021) 2269–2276.
[25] E.T. Luis, A.I. Day, B. König, J.E. Beves, Inorg. Chem. 59 (2020) 9135–9142.
[26] O. Danylyuk, V. Sashuk, CrystEngComm 22 (2020) 2900–2903.
[27] H.J. Kim, J. Heo, W.S. Jeon, et al., Angew. Chem. Int. Ed. 40 (2001) 1526–1529.
[28] W. Gong, X. Yang, P.Y. Zavalij, et al., Chem. Eur. J. 22 (2016) 17612–17618.
[29] X. Yang, R. Wang, A. Kermagoret, D. Bardelang, Angew. Chem. Int. Ed. 59 (2020) 21280–21292.
[30] G. Wu, Z. Huang, O.A. Scherman, Angew. Chem. Int. Ed. 59 (2020) 15963–15967.
[31] K.M. Anis-Ul-Haque, C.E. Woodward, A.I. Day, L. Wallace, Inorg. Chem. 59 (2020) 3942–3953.
[32] M. Liu, L. Chen, P. Shan, et al., ACS Appl. Mater. Inter. 13 (2021) 7434–7442.
[33] Y. Luo, W. Zhang, M. Liu, et al., Chin. Chem. Lett. 32 (2021) 367–370.
[34] Y. Zhang, K. Lu, M. Liu, et al., Dalton Trans. 49 (2020) 404–410.
[35] X. Yang, F. Liu, Z. Zhao, et al., Chin. Chem. Lett. 29 (2018) 1560–1566.
[36] J. Chen, Y. Su, F. Lin, et al., Ecotoxicol. Environ. Saf. 224 (2021) 112711.
[37] B. Parmar, K.K. Bisht, Y. Rachuri, E. Suresh, Inorg. Chem. Front. 7 (2020) 1082–1107.
[38] M. Zhang, X. Yan, F. Huang, Z. Niu, H.W. Gibson, Acc. Chem. Res. 47 (2014) 1995–2005.
[39] J.F. Chen, G. Meng, Q. Zhu, S. Zhang, P. Chen, J. Mater. Chem. C 7 (2019) 11747–11751.
[40] M. Noboru, K. Yozo, K. Masao, Bull. Chem. Soc. Jpn. 29 (1956) 465–470.
[41] K. Li, Y. Liu, Y. Li, et al., Chem. Sci. 8 (2017) 7258–7267.
[42] H. Sun, X.X. Tang, B.X. Miao, Y. Yang, Z. Ni, Sens. Actuat. B: Chem. 267 (2018) 448–456.
[43] L. Yang, H. Yang, F. Li, X. Zhang, Langmuir 29 (2013) 12375–12379.
[44] Y. Jiao, J.F. Xu, Z. Wang, X. Zhang, ACS Appl. Mater. Interfaces 9 (2017) 22635–22640.